Universality of critically pinned interfaces in 2-dimensional isotropic random media

Peter Grassberger[1]
[1] *JSC, FZ Jülich, D-52425 Jülich, Germany*
(Dated: March 13, 2022)

Based on extensive simulations, we conjecture that critically pinned interfaces in 2-dimensional isotropic random media with short range correlations are always in the universality class of ordinary percolation. Thus, in contrast to interfaces in > 2 dimensions, there is no distinction between fractal (i.e., percolative) and rough but non-fractal interfaces. Our claim includes interfaces in zero-temperature random field Ising models (both with and without spontaneous nucleation), in heterogeneous bootstrap percolation, and in susceptible-weakened-infected-removed (SWIR) epidemics. It does not include models with long range correlations in the randomness, and models where overhangs are explicitly forbidden (which would imply non-isotropy of the medium).

arXiv:1711.02904v2 [cond-mat.dis-nn] 12 Nov 2017

Interfaces between different phases are important in many fields of physics, material sciences, and biology. One might just mention boundaries of magnetic domains, cell membranes, or combustion fronts. Because of that, there exists a huge literature [1, 2]. Maybe best understood are moving interfaces (the most famous model there being that of Kardar, Paris, and Zhang [3]), but in the present paper we shall deal with interfaces that, although being pushed, get pinned at random obstacles. More precisely, we are interested in *critically* pinned interfaces, where the pushing force is just such that the movement gets slower and slower, and would stop at infinite time. We assume that the medium in which the interface moves is isotropic with short range correlations, and we neglect thermal fluctuations. Finally, we will only be interested in 2 dimensions, where the interface is a line.

Since the literature on pinned (and moving) interfaces is dominated by models where overhangs are neglected [4–6], we should stress that such models do *not*, in principle, describe isotropic media. It *may* be that overhangs turn out to be unimportant on large scales, but that is something that should not be imposed from the very beginning. There is a consensus that they are indeed irrelevant for *growing* interfaces, but the situation is much less clear for pinned interfaces – and, in particular, in two dimensions. Therefore, overhangs will in the following be fully taken into account.

Maybe the oldest and best understood model of such interfaces (although it is often not considered as such) is percolation [7]. The reason why boundaries of critical percolation clusters are usually not considered as interfaces is that these clusters are fractal, and therefore cannot be considered as a (bulk) phase. But this does not take into account the possibility that maybe there are no critically pinned interfaces at all that separate two non-fractal phases, i.e. that interfaces maybe *always* are between fractal phases.

It is well known [8–11] that 2-d interfaces in 3-d random media can be either fractal (as in ordinary percolation, OP) or rough but non-fractal. Indeed, it was shown by Janssen *et al.* [17], that these two cases can be realized in the same model, and are separated by a tricritical point, in any dimension ≥ 3. This was verified numerically in [18], where the tricritical exponents were measured precisely in $d = 3$, and where it was found that no such tricritical point exists for $d = 2$.

If the latter is correct and general, this would mean that critically pinned interfaces in 2-d isotropic media are *always* in the universality class of OP. This had been conjectured before [19], but the opposite was claimed in many, even very recent, papers [12–16, 20–27] In most of these papers [12–16, 20, 26–28] it is claimed that the percolation scenario breaks down when the disorder is weak. But in others [23–25], even in the percolation like phase the critical exponents were found to be different. In [22], even continuously varying exponents were found. In [28], it was correctly claimed that the fractal-to-rough transitions seen in previous papers were finite size effects and that interfaces in the random field Ising model (RFIM) in $d = 2$ are in the percolation universality class, but it was also claimed that the critical field strength for small disorder is zero, which seems to contradict our results. Finally, in [29] exponents were found that are in rough agreement with those for OP, but no connection was suggested.

Indeed, it is known [30] that no phase transitions can exist in Ising-type models with quenched disorder, even at zero temperature. In principle, this should exclude any tricritical point as found by Janssen et al. in higher dimensions, but the situation is somewhat more subtle [31], since the existence of non-fractal pinned interfaces does not necessarily imply that the two phases separated by them are *thermodynamically* stable.

It is the purpose of the present paper to clarify this situation, by means of simulations that show clearly that the transitions proposed in earlier papers were just crossovers that exist only for finite systems, and that the exponents are always those of OP.

The model used in our simulations is the generalization of site and bond percolation introduced in [18]. In this model, the probability that a site surrounded by n

"wetted" (infected, flipped) sites will ultimately also be wetted is q_n. Put differently, if these neighbors "attack" the site in any sequential order, then the probability for the site to fall during the $m-$th attack is p_m with

$$q_n = q_{n-1} + (1 - q_{n-1})p_n : \quad (1)$$

if the site has fallen after n attacks, then either it had already fallen before the last one, or (if not) it falls during the last. Site percolation corresponds to $p_1 = p, p_m = 0$ for $m > 1$. Bond percolation has $p_m = p$ for all m.

The simplest non-trivial model in this class, called the "minimal model" (MM) in the following, has $p_m = p_2$ for all $m > 2$. In this model one just has to distinguish between first and subsequent attacks, but not between second, third, etc. This is also identical to the SWIR model of [32–35] for the special case where sites get weakened with probability 1 after an attack. The general SWIR model with finite weakening probability has non-trivial p_m's that can easily obtained recursively [38]. Finally, also the heterogeneous k-core percolation model of [36, 37] is equivalent to the above model with general p_m's. This is less obvious, because in [36, 37] sites do not fall with ad hoc determined probabilities, but have probabilities to be in the k-core that were chosen before any spreading. But since each site can get infected at most once, it is easy to see that both points of view are equivalent.

Finally, also the RFIM model is a special case of the above [19]. Consider the Hamiltonian $H = -J\sum\langle i,j\rangle S_iS_j - \sum_i(h_i + H)S_i$ with $S_i = \pm 1$, where we can take $J = 1$ without loss of generality, and where the local fields h_i are distributed according to some probability $P(h)$. In the following, we shall consider explicitly the uniform distribution $P(h) = \Theta(\Delta - |h|)/2\Delta$, and the Gaussian distribution $P(h) = 1/(\sqrt{2\pi}\sigma)\exp[h^2/(2\sigma^2)]$.

Consider the case where we start with a very strong negative external field, $H \ll 0$, so that all spins are initially $S_i = -1$. Then we increase H continuously. A spin i surrounded by n "up" and $\mathcal{N}$ "down" spins ($\mathcal{N}$ is the coordination number; on the square lattice, $\mathcal{N} = 4$) will flip, if this becomes energetically favorable, $H > \mathcal{N} - 2n - h_i$. Therefore,

$$q_n = \int_{\mathcal{N}-2n-H}^{\infty} P(h)dh. \quad (2)$$

The final expressions for uniform and Gaussian distributions are given in [38].

Notice that this gives in general also $q_0 > 0$, i.e. spins can also flip spontaneously without any flipped neighbors, i.e. clusters can nucleate [39]. We have then two options: we can either follow the bulk of the literature on the kinetic zero-temperature RFIM and forbid spontaneous flips *by fiat*, or we can allow them (we do not allow spontaneous flips of multiple spins). In the former case we have to start with a *seed* (we take wither a single point seed or an entire line on which the spins are already flipped initially). In the latter case, we can use the same code, provided we include in the seed those sites that would flip spontaneously. The actual codes used are described in [38].

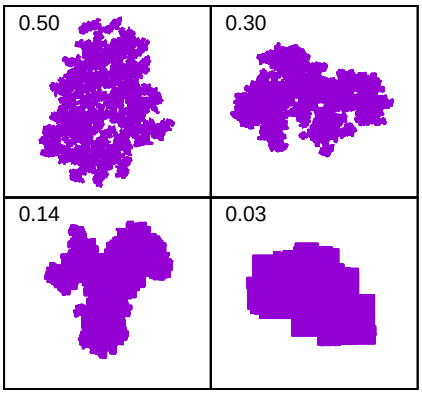


FIG. 1. (color online) Typical critical clusters obtained from single site seeds with the MM. The numbers written in each panel show the values of p_1. The values of p_2 are $0.50, 0.88092, 0.977452$, and 0.99897. The upper left panel corresponds to bond percolation.

Typical critical clusters obtained with the MM are shown in Fig. 1. While the clusters in the upper row are obviously fractal (the left one is indeed bond percolation), the ones in the lower row *seem* to be compact. It is this which has misled many authors to claim that the growth is indeed compact when p_1 is small. The reason why the clusters look less fractal for small p_1 is clear: small a_1p and large p_2 mean that growth into new territory is slowed down, while bays and fjords are filled up.

The fact that this seeming compactness is only transient is best seen by studying the usual observables for percolation growth: The number $N(t)$ of growth sites at time t, the survival probability $P(t)$, and the r.m.s. distance $R^2(t)$ of the growth sites from the seed. The scaling laws for OP are summarized in [38].

In Fig. 2 we show $N(t)/P(t)$ for $p_1 = 0.1$ and for several values of p_2 close to $p_{2,c}$. We see the expected huge deviations from scaling for small t, but for $t > 10^4$ there is one straight curve, and it has precisely the exponent of the percolation universality class. This might be an accident, but as seen from Fig. 3, the same value of p_2 gives also power laws for $P(t)$ and $R^2(t)$ with exactly the right critical exponents. Blow-ups of these figures, where we have also divided the data by the expected power laws to obtain horizontal curves at criticality, are given in [38].

Similar analyses were also made for 30 other values of p_1, in the range $0.03 \le p_1 \le 0.592746$. For each of them we obtained q_c with errors $\approx 10^{-5}$, see Fig. 4 (remember

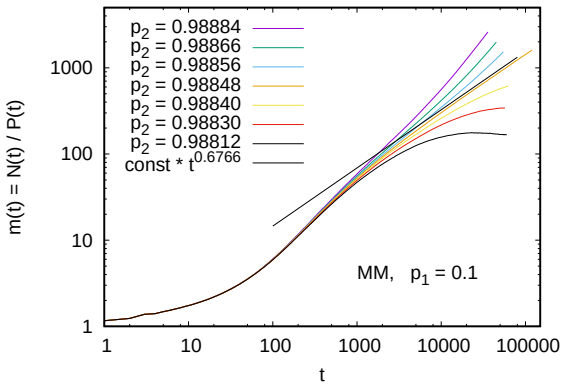


FIG. 2. (color online) Log-log plot of the average number of growth sites per surviving cluster in the MM, plotted against time t. Each curve corresponds to a different value of p_2, while $p_1 = 0.1$ is common to all curves. The straight line has the slope expected for OP.

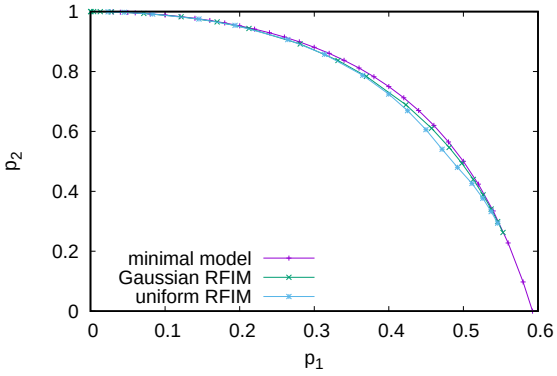
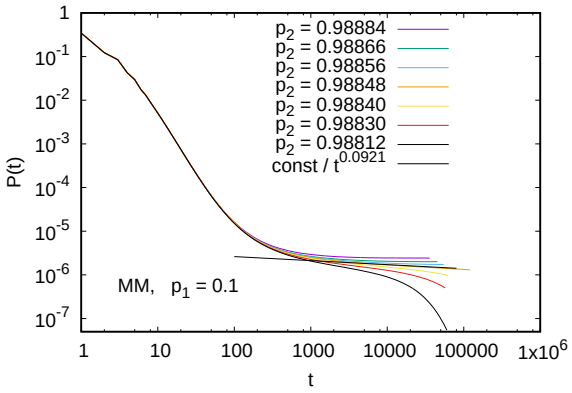


FIG. 4. (color online) Phase boundaries for the minimal model and for two versions of the RFIM. Interfaces are moving in the region above the curves, and pinned below. Error bars on all points are much smaller than the symbols.



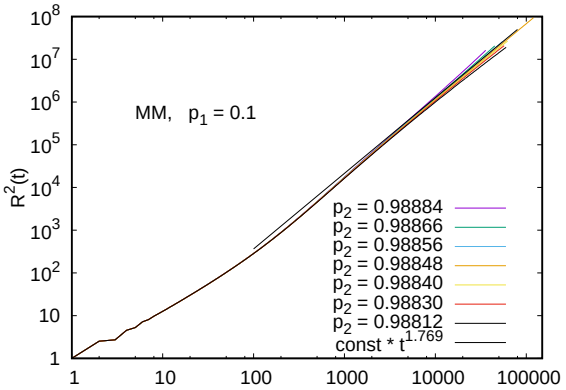


FIG. 3. (color online) Similar to Fig. 2, but for the survival probability $P(t)$ (top panel) and for $R^2(t)$ (bottom panel).

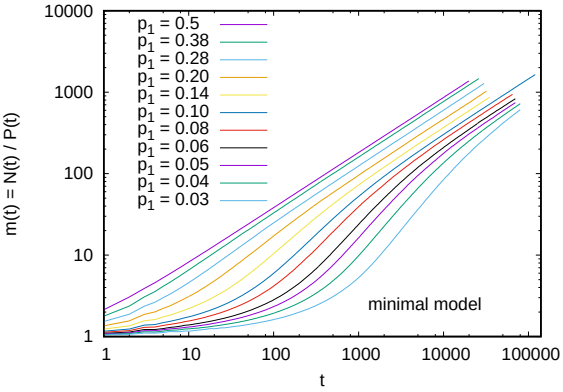


FIG. 5. (color online) Log-log plots of $m(t) = N(t)/P(t)$ for $p_2 = p_{2,c}(p_1)$, i.e. on the critical curve. For small p_1, clusters hardly grow at the beginning, but the long time growth is that of OP.

that $p = p_1$ and $q = p_2$ for the MM). Some of the critical curves of $N(t)/P(t)$ versus t are shown in Fig. 5. They show increasingly large deviations from scaling as $p \to 0$, but they all show the scaling of ordinary percolation for large t. The deviations at small t arise from the fact that only very clusters survive the initial growth phase, and even if they do they grow very slowly. In the limit $p \to 0$, each surviving cluster is just a single site that performs a self-avoiding random walk. All this is clearly seen from plots analogous to Fig. 4, but for $P(t)$ and $R^2(t)$ [38].

Let us now turn to line seeds, i.e. to initially flat interfaces. The decrease of the number of growth sites with time is shown in Fig. 6, for critically pinned interfaces

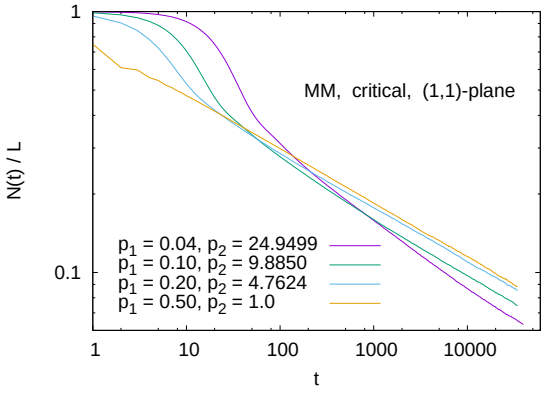


FIG. 6. (color online) Log-log plots of $N(t)/L$ for critical interfaces with global (1,1) orientation.

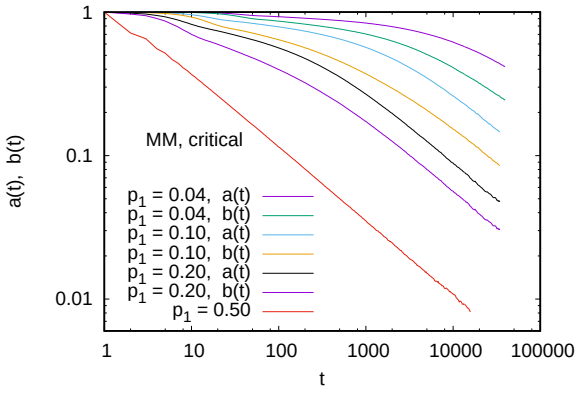


FIG. 7. (color online) Log-log plots of asymmetries $a(t)$ and $b(t)$ for critical interfaces with global (1,1) orientation. Notice that $a(t) = b(t)$ by definition for bond percolation.

with (1,1) orientation. We see precisely the expected power laws [38] for large t, preceded for small p by initial periods where $N(t) \approx const$. Data for interface heights are shown in [38].

For a last check that the MM is in the OP universality class, we studied the *local* orientation of globally flat interfaces. Local orientations are measured by the directions of either *attacks*, i.e. any contacts between infected and susceptible sites, or *infections*, i.e. such contacts that lead actually to an infection of the immune site [40, 41]. Let us define m_f and m_b as the number of forward and backward attacks/infections, and

$$a(t) = \frac{m_{f,\text{attack}} - m_{b,\text{attack}}}{m_{f,\text{attack}} + m_{b,\text{attack}}}, b(t) = \frac{m_{f,\text{infect}} - m_{b,\text{infect}}}{m_{f,\text{infect}} + m_{b,\text{infect}}}. \quad (3)$$

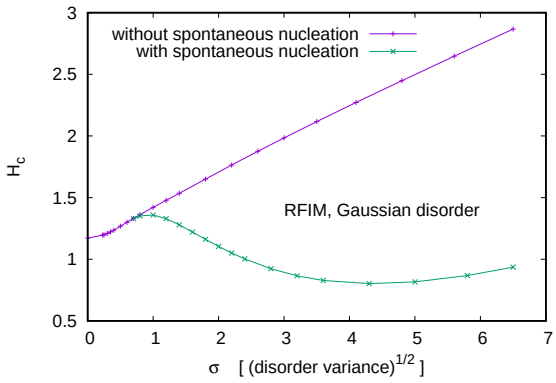


FIG. 8. (color online) Depinning thresholds for the RFIM with Gaussian disorder. The value for $\sigma \to 0$ is an exact analytic result [19], the other points are from simulations and have error bars much smaller than the symbols.

It was shown in [40] that these should in general satisfy power laws with new critical exponents, and it is shown in [41] that $a(t) = b(t) \sim t^{-0.5189(1)}$ for OP. Data for $a(t)$ and $b(t)$ for the MM are shown in Fig. 7, where all curves show indeed for large t the expected scaling.

The discussion of the RFIM can now be very short: For all observables, we found very similar behavior, to the point that showing these results is hardly of any use in most cases (some data are shown in [38]). We just have to remember that we can, for any H and any disorder strength, determine the corresponding p_m. Critical values of p_1 and p_2 for the case without spontaneous nucleation are shown in Fig. 4 together with the values for the MM. They are very similar. Both RFI models converge to site percolation ($p_1 = 0.5927\ldots, p_2 = 0$) along the same curve for strong disorder, and behave exactly like the MM for weak disorder (where $q_n = 1$ for $n > 2$).

The only model demanding more discussions is the RFIM with spontaneous nucleation. For weak uniform disorder and not too large H, single sites cannot flip spontaneously. In that case, the simulations where nucleation is forbidden represent the true non-equilibrium RFIM. This is not so for Gaussian disorder, where spontaneous single spin flips can always occur. They are very rare for small disorder, but they become important and change the phase boundary completely for large disorder, see Fig. 8. The most striking aspect of this plot is the huge difference with the results of [28], who found much smaller values of H_c, and conjectured $H_c = 0$ for $\sigma < 0.6$. Presumably this is due to the fact that we allowed only single spin spontaneous flips, while the states in [28] were stable against flips of *any* finite clusters. We checked that flipping clusters with two-site seeds did not change our results, but flipping larger clusters with larger

seeds would have been impossible with our algorithm.

Let us finally comment on facetted growth, as seen e.g. in [8, 9, 12–15]. Obviously, this cannot occur in strictly isotropic media, since it requires a regular lattice for the orientations of the facets (notice that we also discussed lattice models in this paper, but Fig. 7 showed that indeed the lattice anisotropy became irrelevant in the scaling limit). In addition, it seems that facetted growth never is critical. In [38] we discuss this for the RFIM with uniform disorder, where a first order transition was claimed in [22, 29].

In summary, we found numerically that in all models the depinning transition is in the ordinary percolation universality class. In [42, 43] it was also found that interfaces in a 2-d SIR type model of coinfections are in the OP class (in contrast to higher dimensions). Together with analytical arguments this gives strong support to our more general claim. It also suggests that a percolative phase transition in a 2-d model with intermediate length dependency links [44] is continuous and in the OP class, as claimed in[45] and in contrast to claims made in [44].

Acknowledgements: I thank Golnoosh Bizhani and Maya Paczuski for collaborations during very early stages of this work.

[1] F. Family and T. Viscek, *Dynamics of Fractal Surfaces*, World Scientific, Singapore 1991.

[2] A.L. Barabasi and H.E. Stanley, *Fractal concepts in surface growth*, Cambridge Univ. Press, Cambridge 1995.

[3] M. Kardar, G. Parisi, and Y.C. Zhang, Phys. Rev. Lett. **57**, 1810 (1986).

[4] T. Nattermann, S. Stepanow, L.-H. Tang, and H. Leschhorn, J. Phys. II (France) **2**, 1483 (1992).

[5] T. Giamarchi and P. Le Doussal, Phys. Rev. B **52**, 1242 (1995).

[6] P. Le Doussal, K.J. Wiese, and P. Chauve, Phys. Rev. B i*66*, 174201 (2002).

[7] D. Stauffer and A. Aharony, *Introduction to percolation theory*, Taylor & Francis, London 1994.

[8] H. Ji and M.O. Robbins, Phys. Rev. B **46**, 14519 (1992).

[9] B. Koiller, H. Ji, and M. O. Robbins, Phys. Rev. B **45**, 7762 (1992);

[10] B. Koiller, H. Ji, and M. O. Robbins, **46**, 5258 (1992);

[11] B. Koiller and M.O. Robbins, Phys. Rev. B **62**, 5771 (2000).

[12] M. Cieplak and M.O. Robbins, Phys. Rev. Lett. **60**, 2042 (1988);

[13] M. Cieplak and M.O. Robbins, Phys. Rev. B **41**, 11508 (1990);

[14] N. Martys, M. Cieplak, and M.O. Robbins, Phys. Rev. Lett. **66**, 1058 (1991);

[15] N. Martys, M.O. Robbins, and M. Cieplak, Phys. Rev. B **44**, 12294 (1991);

[16] C.S. Nolle, B. Koiller, N. Martys, and M.O. Robbins, Phys. Rev. Lett. **71**, 2074 (1993);

[17] H.-K. Janssen, M. Müller, and O. Stenull, Phys. Rev. E **70**, 026114 (2004).

[18] G. Bizhani, M. Paczuski, and P. Grassberger, Phys. Rev. E **86**, 011128 (2012).

[19] B. Drossel and K. Dahmen, Euro. Phys. J. B, **3**, 485 (1998).

[20] C. Frontera and E. Vives, Phys. Rev. E **59**, R1295 (1999).

[21] N.J. Zhou and B. Zheng, Phys. Rev. E **82**, 031139 (2010).

[22] X.P. Qin, B. Zheng and N.J. Zhou, J. Phys. A **45**, 115001 (2012).

[23] Bin Xi, Meng-Bo Luo, Valerii M. Vinokur and Xiao Hu, Scientific Reports **5**, 14062 (2015).

[24] D. Spasojević, S. Janićević, and M. Knezević, Europhys. Lett. **76**, 912 (2006); Phys. Rev. E**84**, 051669 (2011); Phys. Rev. Lett. **106**, 175701 (2011); Phys. Rev. E**89**, 012118 (2014).

[25] S. Janićević, S. Mijatović, and D. Spasojević, Phys. Rev. E**95**, 042131 (2017).

[26] D. Thongjaomayum and P. Shukla, Phys Rev E **88**, 042138 (2013).

[27] L. Kurbah, D. Thongjaomayum and P. Shukla, Phys Rev E **91**, 012131 (2015).

[28] E.T. Seppälä and M.J. Alava, Phys. Rev. E **63**, 066109 (2001).

[29] Lisha Si, Xiaoyun Liao, Nengji Zhou, Comput. Phys. Commun. **209**, 34 (2016).

[30] M. Aizenman and J. Wehr, Commun. Math. Phys. **130**, 489 (1990).

[31] I. Balog, G. Tarjus, and M. Tissier, e-print arXiv:1710.04032 (2017).

[32] K. Chung, Y. Baek, D.Kim, M. Ha, and H. Jeong, Phys. Rev. E **89**, 052811 (2014).

[33] K. Chung, Y. Baek, M. Ha, and H. Jeong, Phys. Rev. E **93**, 052304 (2016).

[34] Deokjae Lee, Wonjun Choi, Janos Kértesz, and Byungnam Kahng, Scientific Reports **7**, 5723 (2017).

[35] Wonjun Choi, Deokjae Lee, Janos Kértesz, and Byungnam Kahng, arXiv:1706/08968 (2017).

[36] G.J. Baxter, S.N. Dorogovtsev, A.V. Goltsev, and J.F.F. Mendes, Phys. Rev. E **83**, 051134 (2011).

[37] D. Cellai, A. Lawlor, K.A. Dawson, and J.P. Gleeson, Phys. Rev. Lett. **107**, 175703 (2011).

[38] supplemental material

[39] For Gaussian disorder with any σ this can happen for any H, but for uniform disorder single spins can flip spontaneously only if $H + \Delta > \mathcal{N}$.

[40] H.-K. Janssen and O. Stenull, J. Phys. A: Math. Theor. **50**, 324002 (2017).

[41] P. Grassberger, to be published.

[42] W. Cai, L. Chen, F. Ghanbarnejad, and P. Grassberger, Nature Physics **11**, 936 (2015).

[43] P. Grassberger, L. Chen, F. Ghanbarnejad, and W. Cai, Phys. Rev. E **93**, 042316 (2016).

[44] W. Li, A. Bashan, S.V. Buldyrev, H.E. Stanley, and S. Havlin, Phys. Rev. Lett. **108**, 228702 (2012).

[45] P. Grassberger, Phys. Rev. E **91**, 062806 (2015).

arXiv:1711.02904v2 [cond-mat.dis-nn] 12 Nov 2017

Supplemental Material: Universality of critically pinned interfaces in 2-dimensional isotropic random media

I. THE SWIR MODEL

The Susceptible-Weakened-Infected-Removed (SWIR) model was defined in [1] as a generalization of the standard Susceptible-Infected-Removed (SIR) model, in which susceptible sites can become weakened with probability μ by infected neighbors, while they get infected with probability κ. Upon further contacts, weakened sites become infected with probability η. Finally, infected sites are removed with probability one.

Let us denote by $p_m(S), p_m(W), p_m(I)$, and $p_m(R)$ the probabilities that an originally susceptible site is in state S, W, I, and R after m contacts. Then we have the recursion

$$\begin{aligned} p_{m+1}(S) &= (1-\kappa-\mu)p_m(S) \\ p_{m+1}(W) &= \mu p_m(S) + (1-\eta)p_m(W) \\ p_{m+1}(I) &= \kappa p_m(S) + \eta p_m(W) \\ p_{m+1}(R) &= p_m(I), \end{aligned} \tag{1}$$

and finally $q_n = p_n(R)$.

II. THE RFIM

In the main text we have seen that the RFIM is a special case of the model of [2], with probabilities q_n given by Eq. (2). For the uniform and Gaussian distributions on the square lattice this gives

$$q_{n,\text{uniform}} = (\Delta + H + 2n - 4)/\Delta \tag{2}$$

and

$$q_{n,\text{gauss}} = \frac{1}{2}\text{erfc}\left(\frac{4-2n-H}{\sqrt{2}\sigma}\right). \tag{3}$$

III. SIMULATIONS

All simulations described in the paper were done with straightforward generalizations of the classical Leath [3] algorithm. In this algorithm one has three data structures:

- A byte map, where for every site its status is stored. In the MM, we have to store for each site only whether it was never attacked, whether it had been attacked, or whether it is removed. For the general SWIR model and for both versions of the RFIM, we have to store also the number of previous attacks. Alternatively, we can also store for each site the number of future attacks at which the site will succumb. The latter of course requires that we determine these numbers in a first pass through the lattice. In contrast, if we store the numbers of past attacks, we can determine when the site falls "on the fly", which is faster if the growing cluster fills only a small part of the lattice. On the other hand, for simulations of the RFIM with spontaneous nucleation, it is more efficient (and simpler) to store the number of future attacks.

- A list of "active" sites. Initially, this contains all seed sites. In later steps (remember that time is discrete) it contains all sites "wetted" (or flipped) in the last previous time step.

- A list of "growth sites". The growth sites at time t are just those neighbors of the sites that were active at time $t-1$, which actually got infected (wetted, flipped). When proceeding from time t to $t+1$, the old list of active sites is replaced by the list of growth sites, and the new list of growth sites starts empty.

Indeed, this describes the "breadth-first" implementation of the Leath algorithm, if we implement the two lists by arrays that are handled in first-in first-out style. Alternatively, we could have implemented them also "depth-first", in which the lists are implemented by stacks handled in first-in last-out style.

While it is in general a matter of taste whether one prefers a breadth-first or a depth-first implementation, the breadth-first one becomes essential for single site seeds and very small q_0. In that case, most attempts to build a large cluster would fail, if the simple Leath algorithm were used, and we used instead a version of PERM (pruned-enhanced Rosenbluth method) [4, 5]. This is based on re-sampling and which allows to grow clusters with good statistics, even if the probability for a cluster to grow is tiny. To be efficient, Leath growth with PERM has to be breadth first [5].

In simulations with single site seeds, we always verified that clusters never reached the lattice boundaries. In simulations with an entire line of seeds, we took this line as one of the four boundaries. Lateral boundary conditions were periodic, while the boundary opposite to the seed was sufficiently far away that the clusters never reached them (this was also checked explicitly). To minimize finite size corrections, we used for the runs with line seeds lattices with aspect ratios ≥ 2, i.e. the lattices were at least twice as long in the lateral direction than in the direction of growth.

Finally, in simulations of the RFIM with spontaneous nucleation, we have to add a last step in order to determine the interface. In these simulations we started with a seed which consists both of a (boundary) line and of all interior sites that would flip spontaneously. After the Leath algorithm is run, the flipped "cluster" consists both of the part that is attached to the line seed, and a large number of disconnected small clusters. In order to remove the latter and to obtain the interface of the connected cluster attached to the line seed, one has to run the Leath algorithm a second time, with only the line as a seed and where only sites are included in the growth that are already flipped after the main step.

Typical lattice sizes were 32678×32678 for single site seeds, and 65536×16384 or 65536×32678 for line seeds. All simulations were done on work station clusters and laptops. The total CPU time spent was about 2 years.

IV. CRITICAL EXPONENTS FOR ORDINARY 2-D PERCOLATION

The "classical" exponents are $\beta = 5/36$, $\nu = 4/3$, and $D_f = 91/48$ [6], where β controls the density of the infinite cluster in the slightly supercritical region, ν controls the divergence of the correlation length as one approaches the critical point, and D_f is the fractal dimension at criticality. In order to compare with the simulations of *growing* clusters as in the present paper, one also needs the minimal path exponent $d_{\min} = 1.13077(2)$ [7], controls the relation between Euclidean distances and "chemical layers" or time. More precisely,

$$R^2(t) \sim t^{2/d_{\min}} \sim t^{1.76871(4)}. \qquad (4)$$

exactly at the critical point. The survival probability $P(t)$ at the critical point scales as

$$P(t) \sim t^{-\delta}, \quad \delta = \beta/(\nu d_{\min}) = 0.092120(2). \qquad (5)$$

Finally, $m(t) = N(t)/P(t)$ is the average number of growth sites per surviving cluster. The sum $M(T) = \sum_{t \le T}$ is then "mass" of a cluster grown for a time T and thus having a radius $R \sim T^{1/d_{\min}}$, and scales as $M \sim R^{D_f} \sim T^{D_f/d_{\min}}$, giving

$$m(t) \sim t^{\mu}, \quad \mu = D_f/d_{\min} - 1 = 0.67659(3). \qquad (6)$$

These are the scaling laws pertinent for single site seeds. For line seeds, the average distance of the growth sites from the seed also scales at criticality as $R \sim t^{1/d_{\min}}$, while the density of the final cluster decays as $\rho(R) \sim R^{D_f - 2}$. Thus the number of growth sites on a lattice of lateral size L should scale as

$$N(t) \sim L t^{-\eta}, \quad \eta = (D_f - 1)/d_{\min} - 1 = 0.20777(1). \qquad (7)$$

The average height of the interface grows, finally, as $h(t) \sim t^{1/d_{\min}}$. This should be independent of the way how we define height. We can use, in particular, the average height of growth sites or we can, for each lateral position x, define height as the maximal height of any infected site.

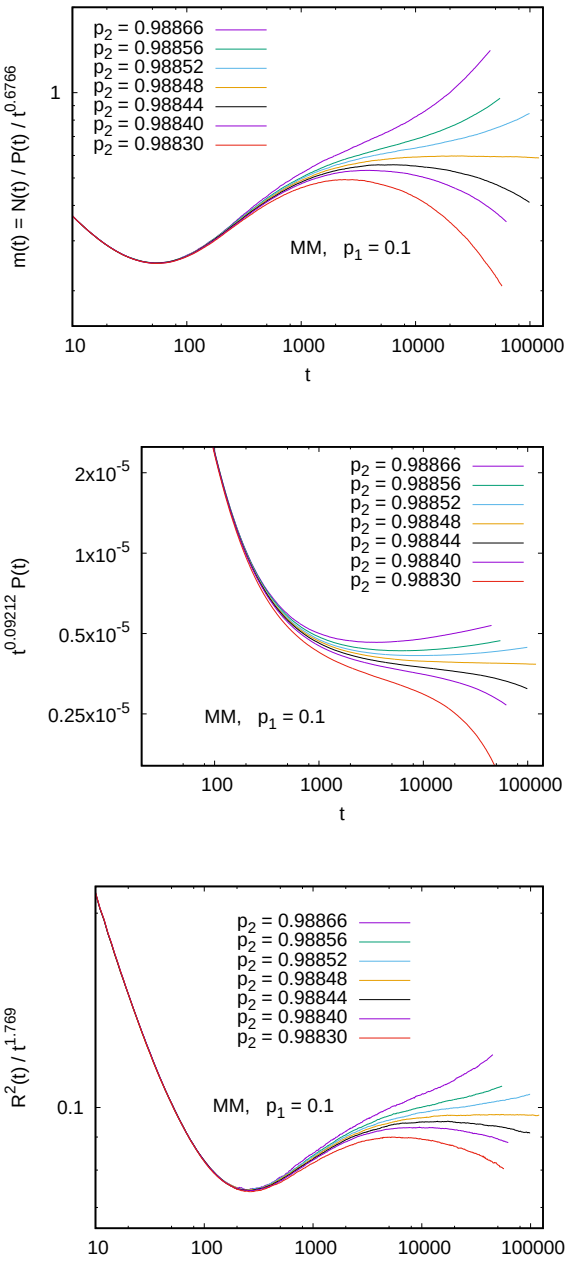


FIG. 1. (color online) Same data as in Figs. 2 and 3 in the main text, but divided by the expected power laws so that the critical curves become horizontal asymptotically.

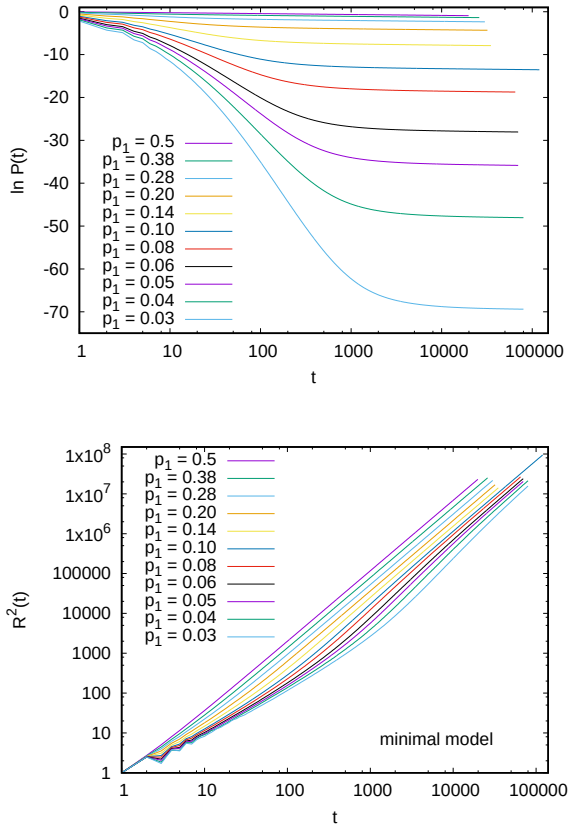


FIG. 2. (color online) Plots of $\ln P(t)$ (upper panel) and $R^2(t)$ (lower panel) against t, for the same 11 points on the critical pinning line for which $N(t)/P(t)$ is shown in Fig. 5 of the main text.

V. POINT SEED CLUSTERS FOR THE MM

In Fig. S1 we show the large-t data (obtained with PERM) shown already in Figs. 2 and 3 of the main text, but multiplied with suitable power laws so that the critical curves are expected to be horizontal, which allows much finer y-axes. We see that indeed the critical curves (corresponding to $p_1 = 0.1, p_2 = 0.988482(2)$) are the most straight for large t and have exactly the exponents expected for percolation.

In Fig. S2 we show $P(t)$ (top panel) and $R^(t)$ (bottom panel) for the same 11 pairs (p, q) as in Fig. 5 of the main text. Thus each curve corresponds to a point on the depinning line. We see that $P(t)$ tends to zero faster than any exponential as $p_1 \to 0$. The best fit for the large-t behavior is

$$P(t) \sim t^{-\delta}\phi(p) \tag{8}$$

with $\phi(p) \sim \exp(-\text{const}/p^{1.1})$ for $p \to 0$, see Fig. S3. The short t behavior of $R^2(t)$ is for $p \to 0$ compatible with a self avoiding random walk of a single-site "cluster".

It was thus easy to verify that the model has for all

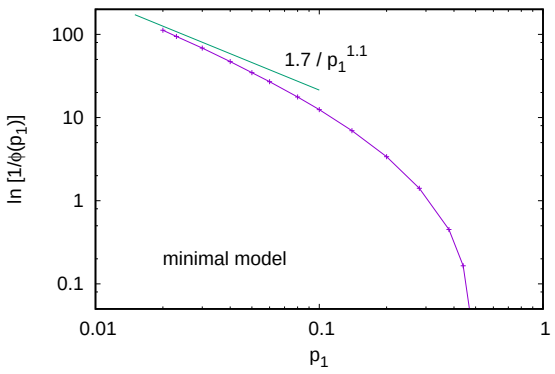


FIG. 3. (color online) Log-log plot of $\ln[1/\phi(p)]$ versus p, where $\phi(p)$ is the prefactor of the power law $P(t) \sim t^{-\delta}$. The straight line corresponds to $\phi(p) = \exp(-1.7/p^{1.1})$.

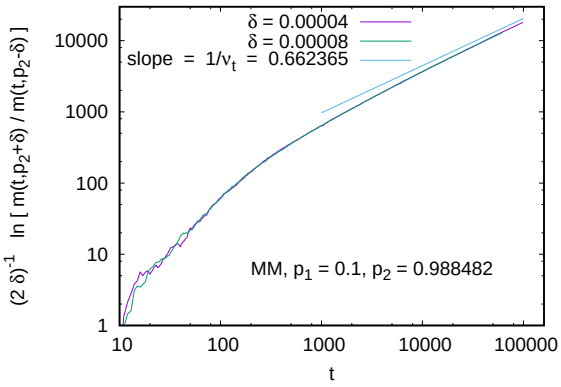


FIG. 4. (color online) Log-log plot of the derivative of $\ln m(t, p_2)$ with respect to p_2, plotted against t. Two estimates of the derivative are provided by finite difference quotients with $\Delta p_2 = 0.00004$ and 0.00008, respectively. The straight line is the scaling expected for OP, with $\nu = 4/3$.

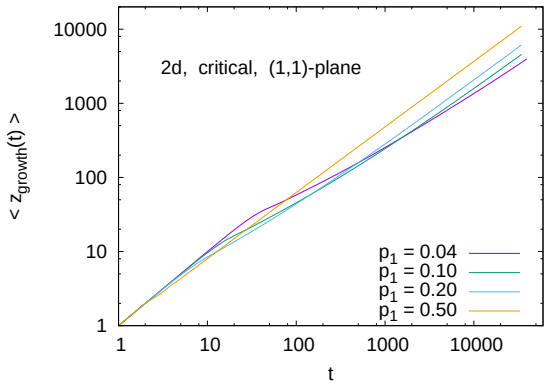


FIG. 5. (color online) Log-log plot of $h(t)$ versus t for critical interfaces of the MM with initial orientation (1,1).

values of p_1 the percolation critical exponents when it is *exactly on* the critical line. But verifying the exponents that control the off-critical behavior (the order parameter exponent β and the correlation length exponent ν turned out to be much more difficult. One reason is the smallness of the critical region when p_1 is small. Another reason is that corrections to scaling seem to be even more important.

One popular way to obtain ν or $\nu_t = \nu d_{\min}$ is by means of data collapse plots. In the present case we would plot $t^{-\mu} m(t)$ against $(p_2 - p_{2,c}) t^x$ for different values of x, and would expect a data collapse when $x = 1/\nu_t$. Due to the strong scaling violations for small t, one would do this only for values of t that seem to be in the scaling region. For $p_1 = 0.1$, Fig. S1 would suggest that a good collapse can be expected for $t > 10^4$. Unfortunately, when this is done, the best estimate for ν_t is about 10 percent smaller than the value for percolation. The reason for this can be seen when plotting

$$\frac{d \ln m(t, p_2)}{dp_2}\Big|_{p_2 = p_{2,c}} \approx \frac{\ln[m(t, p_2 + \epsilon)/m(t, p_2 - \epsilon)]}{2\epsilon} \quad (9)$$

against t. From percolation theory we expect that this should scale as t^{1/ν_t}. As seen from Fig. 4, this is compatible with the data, but these data do not fall strictly on a straight line even for the largest values of t. There is some visible curvature even for $t > 10^4$, and the critical scaling would be observed only for $t > 10^5$. In spite of this difficulty, we believe that our data are fully compatible with the OP universality hypothesis.

VI. LINE SEEDS FOR THE MM

If we want to study originally flat interfaces, we have to use line seeds. For small p and t, the growth depends strongly on the orientation of the seed. For interfaces parallel to one of the coordinate axes, initial growth is extremely slow because its velocity is $\propto p$: The interface can only progress, if a site with a single infected neighbor gets infected. On the other hand, for surfaces in the $(1, 1)$ orientation (diagonal), growth is $\propto q$ and thus maximal. For $p \to 0$, the original speed of growth is 1, and stays ≈ 1 until a finite part of the interface lags because $q < 1$.

Average heights of interfaces with $(1, 1)$ orientation at criticality are shown in Fig. S5, where we defined heights via the heights of growth sites, $h(t) = \langle z_{\text{growth}}(t) \rangle$. We see that indeed $h(t) \approx t$ for small p and $t < 1/p$, but for large t all curves show the expected $h(t) \sim t^{1/d_{\min}}$.

VII. LINE SEEDS FOR THE RFIM

The depinning thresholds for the RFIM with uniformly distributed disorder are shown in Fig. S6. As in the analogous Fig. 8 (main text) for the Gaussian model, the upper curve is for the version where spontaneous spin flips are forbidden, while the lower curve is for the version where single spins can flip. Such flips of isolated spins can occur only, if $H + \Delta > 4$, which is indicated by the straight line in Fig. S6. Therefore the depinning threshold curve for the version with single spin flips must be above this line. It seems to be tangential for it at the point $\Delta = 2.42897(3), H = 4 - \Delta$. The existence of a sharp disorder threshold below which no spins can flip spontaneously is the main qualitative difference with the Gaussian model. Otherwise the curves are very similar. In particular, the depinning threshold curves for the versions with spontaneous spin flips are allowed are non-

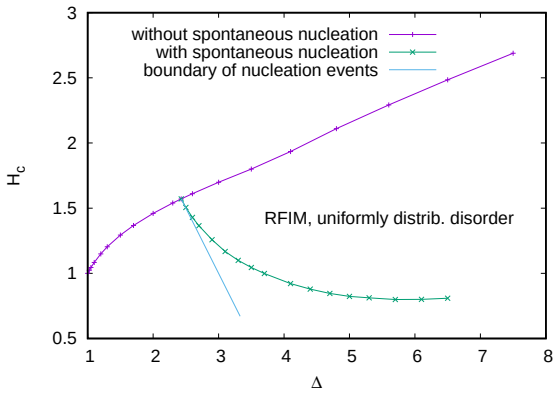


FIG. 6. (color online) Depinning thresholds for the RFIM with uniformly distributed disorder. The value $H_c = 1$ for $\Delta = 0$ is an exact analytic result, the other points are from simulations and have error bars much smaller than the symbols. The straight line indicates the boundary $H + \Delta = 4$, below which no single spins can flip spontaneously.

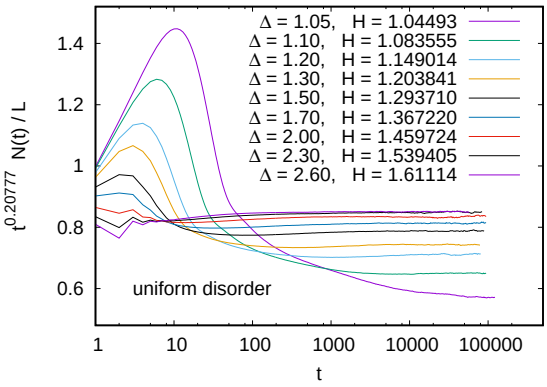


FIG. 7. (color online) Log-linear plot of $t^{0.20777} N(t)/L$ versus t for critical interfaces with initial orientation (1,1), in the RFIM without spontaneous nucleation and with uniform disorder.

monotonic with disorder.

We verified that along both curves in Fig. 8 the exponents are those of critical percolation. This even includes the point $\Delta = 2.42897(3), H = 4 - \Delta$, as far as the exponents δ, μ, η, and $d_{\min}$ are concerned. The exponents β and ν describing off-critical behavior for the version with spontaneous flips are of course different at this point, but they are also as in OP everywhere else.

Finally, we should point out that for uniformly distributed disorder the thresholds depend rather strongly on the sizes of the clusters that are allowed to flip spontaneously. If the dynamics is such that also pairs of adjacent spins can flip, then such flips can flip already for $H + \Delta > 2$, while for any $H + \Delta >$ the probabilities for for flipping large enough clusters are non-zero.

We show here only some of the many data that verify the critical exponents – both for the Gaussian and for the uniform model, and both for with and without single spin flips –, because they are so similar to those for the MM. In Fig. S7 we show, e.g., values of $N(t)/L$ for uniform disorder, at critical values of H. In order to achieve a high resolution on the y-axis, these data are multiplied by $t^{0.20777}$, so that OP scaling would give horizontal curves for large t. We see this is indeed the case, although finite-t corrections are huge for small disorder.

VIII. THE UNIFORM NOISE RFIM WITH $\Delta < 1$

For the RFIM with uniform noise and noise strengh Δ, critically pinned interfaces are in the OP universality class for $\Delta > 1$. As $\Delta \to 1$ from above, also $H_c \to 1$. For $\Delta < 1$, the flipping probability p_1 is non-zero only for $H > 2 - \Delta > 1$. For $1 \le H < 2 - \Delta$, an interface parallel to one of the coordinate axes cannot grow, but since $p_2 \ge 1$ (see Eq. (S2)) any tilted interface can grow with a finite speed that depends on the tilt angle (for (1,1) interfaces the speed is maximal). Finally, the cluster resulting from any finite seed configuration cannot extend out of the convex hull of the seed, since that would require at least one spin with a single flipped neighbor to flip. If, however, the cluster growth is not done in an "epidemic" paradigm, but is done as in invasion percolation [8], the growth of an infinite cluster is enforced and its shape will be a convex polygon, i.e. the interface is facetted. In [9, 10] it is claimed that the growth is "first order" (i.e. discontinuous) for $\Delta < 1$, which is slightly misleading. It is indeed discontinuous for tilted interfaces, but it is continuous for (0,1) interfaces. Indeed, for any originally flat interface there are no overhangs, and the model actually is a simple solid-on-solid model.

[1] K. Chung, Y. Baek, D.Kim, M. Ha, and H. Jeong, Phys. Rev. E **89**, 052811 (2014).

[2] G. Bizhani, M. Paczuski, and P. Grassberger, Phys. Rev. E **86**, 011128 (2012).

[3] P.L. Leath, Phys. Rev. B **14**, 5046 (1976).

[4] P. Grassberger, Comp. Phys. Commun. **147**, 64 (2002).

[5] H.-P. Hsu, W. Nadler, and P. Grassberger, J. Phys. A: Math. Gen. **38**, 775 (2005).

[6] D. Stauffer and A. Aharony, *Introduction to percolation theory*, Taylor & Francis, London 1994.

[7] Zongzheng Zhou, Ji Yang, Youjin Deng, and Robert M. Ziff, Phys. Rev. E **86**, 061101 (2012).

[8] D. Wilkinson and J. F. Willemsen, J. Phys. A: Math. Gen. **16**, 3365 (1983).

[9] X.P. Qin, B. Zheng and N.J. Zhou, J. Phys. A **45**, 115001 (2012).

[10] Lisha Si, Xiaoyun Liao, Nengji Zhou, Comput. Phys. Commun. **209**, 34 (2016).